

Outage Probability Analysis of RF/FSO-VLC Communication Relaying System

Milica Petkovic
University of Novi Sad
Faculty of Technical Sciences
Novi Sad, Serbia
Email: milica.petkovic@uns.ac.rs

Aleksandra Cvetkovic
University of Nis
Faculty of Electronic Engineering
Nis, Serbia
Email: aleksandra.cvetkovic@elfak.ni.ac.rs

Milan Narandzic
University of Novi Sad
Faculty of Technical Sciences
Novi Sad, Serbia
Email: orange@uns.ac.rs

Abstract—This paper presents an analysis of the asymmetric relaying system which provides communication between hybrid outdoor sub-system and indoor visible light communications (VLC) access points. The outdoor sub-system represents a hybrid radio-frequency (RF)/free-space optical (FSO) system, introduced to reduce the impact of weather conditions on transmission quality. Closed-form outage probability analytical expression is derived. Numerical results are presented and confirmed by Monte Carlo simulations. The effects of system and channel parameters on the outage probability performance are investigated and discussed. Greater optical transmitted power of the VLC sub-system reflects in better system performance, as well as lower indoor environment height. When the indoor room is higher, the propagation of the optical signal is longer, and there will be greater power dissipation and performance deterioration. In addition, the outage probability floor is noticed, which is important limiting factor for relaying system design.

I. INTRODUCTION

The optical wireless communication (OWC) is a modern, attractive communication technique, which receives an attention due to benefits of both wireless and optical technologies. The OWC systems are licence-free and low cost, offering high data-rates and very secured transmission. The OWC finds its applications in many areas, such as short-distance interconnects on integrated circuits, indoor communications, terrestrial outdoor links, satellite links, etc. [1]–[3].

The indoor OWC systems, also known as visible light communications (VLC), represent the transmission of the optical signal from visible spectrum. The VLC systems often employ light emitting diodes (LEDs), for both illumination and data communications [2]–[5]. As the OWC application refers to the outdoor environments, the free-space optics (FSO) represents terrestrial point-to-point link, which usually employs laser optical source to perform transmission in infra-red band. The FSO systems represent highly-secured and low-cost wireless transmission. But, the application of the FSO systems is limited by line-of-sight (LOS) requirement, as well as weather and turbulence conditions of the atmospheric channel [1]–[3].

Recently, Gupta *et al.* [6] presented a statistical analysis of the cascaded relaying FSO-VLC system, where the information is delivered to the end users via indoor multiple VLC access points. Motivated by this study, we expand the analysis with the fact that the outdoor FSO link is highly sensitive on conditions of the atmospheric medium. It is known that the

quality of the FSO signal transmission is highly dependent on the visibility, thus it is adversely impacted by fog. On the other hand, the RF transmission is little impacted by fog and mostly affected by rain [2], [3]. For that reason, we consider the first sub-system to be hybrid RF/FSO link [7], [8], employing selection combining (SC) diversity technique to select active link. Hence, the realization of the outdoor signal transmission is dependent on the RF and FSO channel states, which show different sensitivity to snow and rain. The indoor traffic is managed by multiple VLC access points, which distribute data to the end mobile users. Each end user is connected with a single VLC access point, which provides the best channel gain for considered user. The decode-and-forward (DF) relay is assumed to integrate hybrid RF/FSO link and indoor VLC access points. For considered system, the outage probability analytical expression is derived, in order to perform analysis of the system and channel parameters on the transmission quality. Derived expression is utilized to obtained numerical results, which are further validated by Monte Carlo simulations.

The rest of the paper is organized as follows. Section II presents the system and channel model. The outage probability analysis is given in section III, while numerical results are shown in section IV. Some concluding remarks are listed in section V.

II. SYSTEM AND CHANNEL MODEL

As it is shown in Fig. 1, the first part of asymmetric relaying system represents the hybrid RF/FSO sub-system,

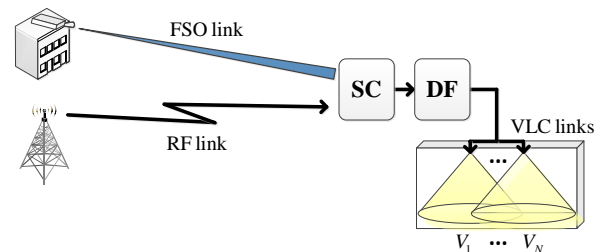


Fig. 1. System model of a RF/FSO-VLC system: SC selects between RF and FSO, DF relay decodes data and forwards it to all VLC LED sources.

with SC spatial diversity technique that processes only the one of the link outputs. The active link will be the one with better channel conditions (greater signal-to-noise ratio (SNR)), i.e., the selection of the active link is dependent on weather conditions. The DF relay performs retransmission on the visible light frequency via N VLC access points placed in some indoor environment. The multiple LEDs, denoted by V_n , $n = 1, \dots, N$, are positioned on the ceiling of the room to transmit the information data to the end users, which are uniformly distributed over the coverage area of the room.

The fading over the RF channel experiences Rayleigh distribution. Thus the instantaneous SNR, γ_{RF} , is exponentially distributed random variable with the probability density function (PDF) given by [9]

$$f_{\gamma_{RF}}(\gamma) = \frac{1}{\mu_1} e^{-\frac{\gamma}{\mu_1}}, \quad (1)$$

where μ_1 is the average SNR over RF link. The cumulative density function (CDF) of the instantaneous SNR, γ_{RF} , is given by [9]

$$F_{\gamma_{RF}}(\gamma) = 1 - e^{-\frac{\gamma}{\mu_1}}. \quad (2)$$

Furthermore, it is assumed that the intensity fluctuations of the received optical signal are modeled by Gamma-Gamma distribution, convenient in wide range of atmospheric turbulence conditions. Thus, the PDF of the instantaneous SNR, γ_{FSO} , is defined as [7]

$$f_{\gamma_{FSO}}(\gamma) = \frac{(\alpha\beta)^{\frac{\alpha+\beta}{2}} \gamma^{\frac{\alpha+\beta}{4}-1}}{\Gamma(\alpha)\Gamma(\beta)\mu_2^{\frac{\alpha+\beta}{4}}} K_{\alpha-\beta} \left(2\sqrt{\alpha\beta\sqrt{\frac{\gamma}{\mu_2}}} \right), \quad (3)$$

where $\Gamma(\cdot)$ is the gamma function defined by [10, (8.310.1)], $K_\nu(\cdot)$ is the ν -th order modified Bessel function of the second kind defined by [10, (8.432.2)], and μ_2 represents the electrical SNR over FSO link. With assumption of the Gaussian plane wave propagation and zero inner scale, the parameters α and β are defined as $\alpha = (\exp[0.49\sigma_R^2(1 + 1.11\sigma_R^{12/5})^{-7/6}] - 1)^{-1}$ and $\beta = (\exp[0.51\sigma_R^2(1 + 0.69\sigma_R^{12/5})^{-5/6}] - 1)^{-1}$, where the Rytov variance, denoted by σ_R^2 , is used as a metric for atmospheric turbulence strength [1], [2].

The corresponding CDF of γ_{FSO} is given by [7]

$$F_{\gamma_{FSO}}(\gamma) = \frac{1}{\Gamma(\alpha)\Gamma(\beta)} G_{1,3}^{2,1} \left(\alpha\beta\sqrt{\frac{\gamma}{\mu_2}} \mid \alpha, \beta, 0 \right), \quad (4)$$

where $G_{p,q}^{m,n}(\cdot)$ is the Meijer's G -function [10, (9.301)].

The instantaneous SNR of the hybrid RF/FSO sub-system, i.e., SNR at the SC output, is defined as

$$\gamma_1 = \max(\gamma_{RF}, \gamma_{FSO}), \quad (5)$$

while the CDF of γ_1 is determined as

$$F_{\gamma_1}(\gamma) = F_{\gamma_{RF}}(\gamma) F_{\gamma_{FSO}}(\gamma), \quad (6)$$

where the CDFs $F_{\gamma_{RF}}(\gamma)$ and $F_{\gamma_{FSO}}(\gamma)$ are previously defined in (2) and (4), respectively.

Regarding the indoor VLC sub-system, it is assumed that the energy of LOS component is greater than the energy of all reflected signals [2], [5]. The reflected signals can be ignored,

thus every end user accepts only the strongest signal sent from all N LEDs. Further, the optical signal transmission to end user is performed by one of N VLC links, which has the best channel conditions. The intercell interferences received from other LEDs are approximated with additive Gaussian process [6], [11].

The LED transmitter is placed at height L from the m -th end user, with the angle of irradiance θ_m , the angle of incidence ψ_m , and radius r_m on the polar coordinate plane, as it can be observed in Fig. 2. The Euclidean distance between the VLC access point and the m -th photodetector receiver is denoted by d_m . Furthermore, the semi-angle at the half-illuminance of LED, $\Phi_{1/2}$, is in relation with the maximum radius of a LED cell footprint, r_e , as $r_e = L \sin(\Phi_{1/2}) / \cos(\Phi_{1/2})$. The order of Lambertian emission is defined as [2], [5], [12]

$$m_l = -\frac{\ln 2}{\ln(\cos \Phi_{1/2})}. \quad (7)$$

The channel gain of the LOS link between LED and the m -th end user terminal is given by [5], [12]

$$I_m = \frac{A(m_l + 1) \Re}{2\pi d_m^2} \cos^{m_l}(\theta_m) Tg(\psi_m) \cos(\psi_m), \quad (8)$$

where A is a photodetector physical surface area, \Re represents a photodetector responsivity, T is the gain of the optical filter, and $g(\psi_m)$ the optical concentrator defined as [11]

$$g(\psi_m) = \begin{cases} n^2 / \sin^2(\Psi), & 0 \leq \psi_m \leq \Psi \\ 0, & \psi_m > \Psi \end{cases}, \quad (9)$$

where n is the refractive index of lens at a photodetector and the field of view (FOV) of the photodetector receiver is Ψ . With assumption that the surface of photodetector receiver is parallel to the ground, as well as that photodetector receiver has no orientation towards the LED, it holds that $\theta_m = \psi_m$.

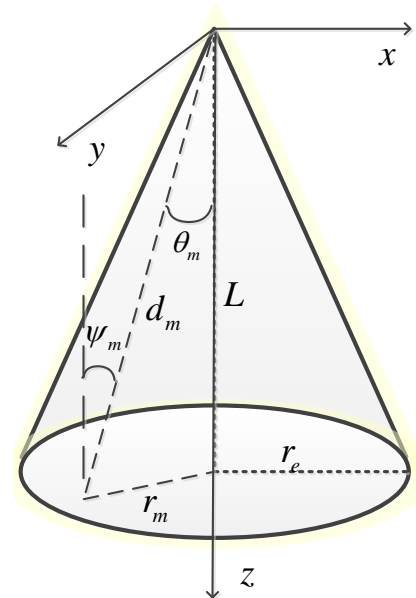


Fig. 2. Geometry of the LOS VLC propagation model

Based on relations $d_m = \sqrt{r_m^2 + L^2}$, and $\cos(\theta_m) = \frac{L}{\sqrt{r_m^2 + L^2}}$, $\mathfrak{S} = \frac{A(m_l+1)\Re}{2\pi} Tg(\psi_m) L^{m_l+1}$ observed in Fig. 2, the channel gain is rewritten as

$$I_m = \frac{\mathfrak{S}}{(r_m^2 + L^2)^{\frac{m_l+3}{2}}}. \quad (10)$$

Under the assumption that user position is random over circular area, the radial distance is modeled by a uniform distribution with the PDF

$$f_{r_m}(r) = \frac{2r}{r_e^2}, \quad (11)$$

defined in $0 \leq r \leq r_e$, while the PDF of the channel gain I_m is derived as

$$f_{I_m}(I) = \frac{2}{r_e^2(m_l+3)} \mathfrak{S}^{\frac{2}{m_l+3}} I^{-\frac{m_l+5}{m_l+3}}, \quad (12)$$

defined in $I \in [I_{\min}, I_{\max}]$, where $I_{\min} = \frac{\mathfrak{S}}{(r_e^2+L^2)^{\frac{m_l+3}{2}}}$ and $I_{\max} = \frac{\mathfrak{S}}{L^{m_l+3}}$. The instantaneous SNR of the VLC channel of the m -th end user can be defined as

$$\gamma_{VLC_m} = \frac{P_t^2 \eta^2 I_m^2}{N_0 B}, \quad (13)$$

where P_t is transmitted optical power of each LED, η is an optical-to-electrical conversion efficiency, N_0 denotes noise spectral density, and B the baseband modulation bandwidth.

Based on (12) and (13), considering $\mu_{VLC} = \frac{P_t^2 \eta^2}{N_0 B}$, the PDF of the instantaneous SNR of the m -th end user is derived as

$$f_{\gamma_{VLC_m}}(\gamma) = \frac{\mu_{VLC}^{\frac{1}{m_l+3}} \mathfrak{S}^{\frac{2}{m_l+3}}}{r_e^2(m_l+3)} \gamma^{-\frac{m_l+4}{m_l+3}}, \quad (14)$$

defined in $\gamma \in [\gamma_{\min}, \gamma_{\max}]$, where $\gamma_{\min} = \frac{\mu_{VLC} \mathfrak{S}^2}{(r_e^2+L^2)^{\frac{m_l+3}{2}}}$ and $\gamma_{\max} = \frac{\mu_{VLC} \mathfrak{S}^2}{L^{2(m_l+3)}}$. The corresponding CDF of the instantaneous SNR of the m -th end user is derived as

$$F_{\gamma_{VLC_m}}(\gamma) = 1 + \frac{L^2}{r_e^2} - \frac{\mathfrak{S}^{\frac{2}{m_l+3}}}{r_e^2} \left(\frac{\gamma}{\mu_{VLC}} \right)^{-\frac{1}{m_l+3}}. \quad (15)$$

The VLC link that performs the optical signal transmission will be established between the mobile user and the closest LED. With assumption that all VLC links are independent and identically distributed random variables, the CDF of the best instantaneous SNR regarding the m -th end user, denoted by γ_2 , is

$$F_{\gamma_2}(\gamma) = [F_{\gamma_{VLC_m}}(\gamma)]^N, \quad (16)$$

where $F_{\gamma_{VLC_m}}(\gamma)$ is the CDF of the instantaneous SNR of the VLC link between the n -th LED and the m -th end user defined in (15).

III. OUTAGE PROBABILITY ANALYSIS

For asymmetric DF based RF/FSO-VLC system, the equivalent end-to-end SNR at the m -th end user is defined as

$$\gamma_{eq} = \min(\gamma_1, \gamma_2), \quad (17)$$

where γ_1 is the instantaneous SNR of the hybrid RF/FSO subsystem and γ_2 is the instantaneous SNR of the active VLC link. The outage probability for a single end user is determined as the probability that γ_{eq} falls below a predetermined outage protection value, γ_{th} , which can be written as

$$P_{out} = \Pr[\gamma_{eq} < \gamma_{th}] = \Pr[\min(\gamma_1, \gamma_2) < \gamma_{th}] \\ = F_{\gamma_1}(\gamma_{th}) + F_{\gamma_2}(\gamma_{th}) - F_{\gamma_1}(\gamma_{th}) F_{\gamma_2}(\gamma_{th}), \quad (18)$$

where the CDFs $F_{\gamma_1}(\cdot)$ and $F_{\gamma_2}(\cdot)$ are previously defined in (6) and (16), respectively.

IV. NUMERICAL RESULTS AND DISCUSSIONS

In this section, numerical results are presented and validated by Monte Carlo simulations. The values of the system and channel parameters are given in Table I [12], [13]. Numerical results are obtained based on the outage probability expression in (18), which includes the CDF expressions presented in (6) and (16).

The outage probability in the function of $\mu_1 = \mu_2$ is presented in Fig. 3 for two system scenarios. Besides considered system where the first part is hybrid RF/FSO system, the results for scenario analyzed in [6] are also presented, referring to the case where the first sub-system includes only a single FSO link. Weak ($\sigma_R^2 = 0.25$) or strong ($\sigma_R^2 = 2$) atmospheric turbulence conditions are considered. From presented results, it is clear that the system performance can be significantly improved by introducing the RF link as a backup link for the FSO system. This improvement is highly expressed when the FSO link suffers from strong atmospheric turbulence. For example, if $\mu_1 = \mu_2 = 25$ dB, by adding the RF link besides the FSO one with SC technique, the outage probability is improved about 58 times when $\sigma_R^2 = 0.25$, while about 313 times when $\sigma_R^2 = 2$.

Fig. 4 presents the outage probability dependence on $\mu_1 = \mu_2$ when the FSO link is affected by different atmospheric turbulence conditions. The number of the VLC

TABLE I
Constants and system parameters

name	symbol	value=
photodetector surface area	A	1 cm ²
responsivity	\Re	0.4 A/W
optical filter gain	T	1
refractive index of lens at a photodetector	n	1.5
FOV of receiver	Ψ	60°
optical-to-electrical conversion efficiency	η	0.8
noise spectral density	N_0	10 ⁻²¹ W/Hz
Rytov variance for weak		
atmospheric turbulence condition	σ_R^2	0.25 (< 1)
Rytov variance for strong		
atmospheric turbulence condition	σ_R^2	2 (> 1)

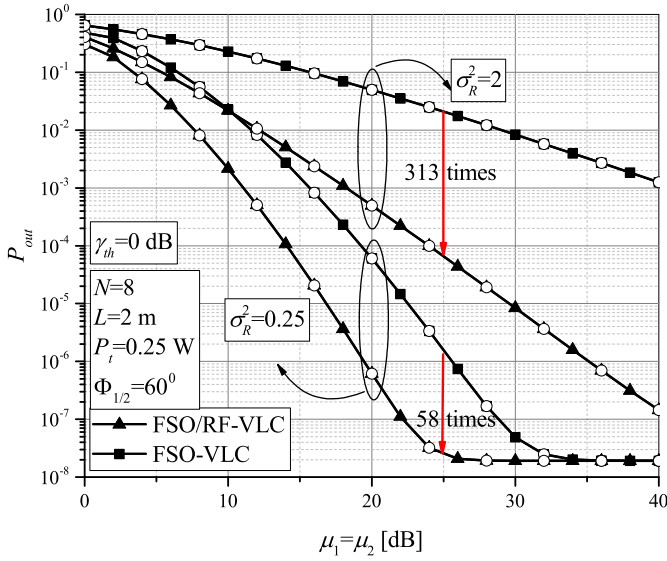


Fig. 3. Outage probability for RF/FSO-VLC and FSO-VLC systems in various atmospheric turbulence strengths

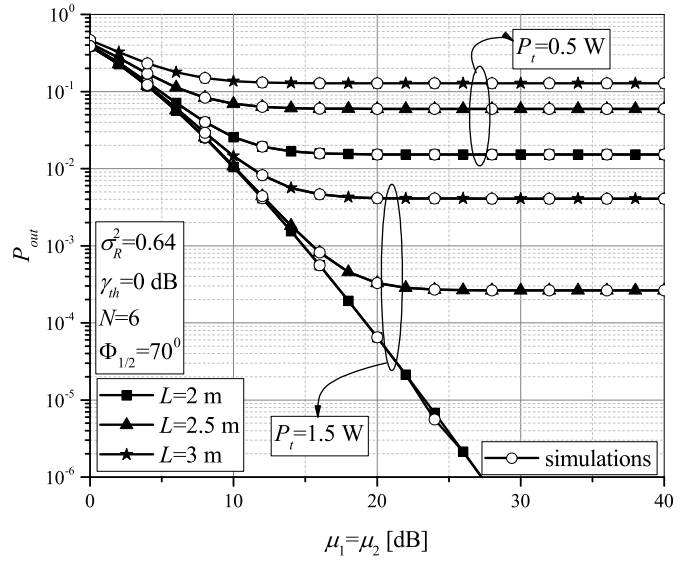


Fig. 5. Outage probability vs. $\mu_1 = \mu_2$ for different transmitted optical power and different room heights

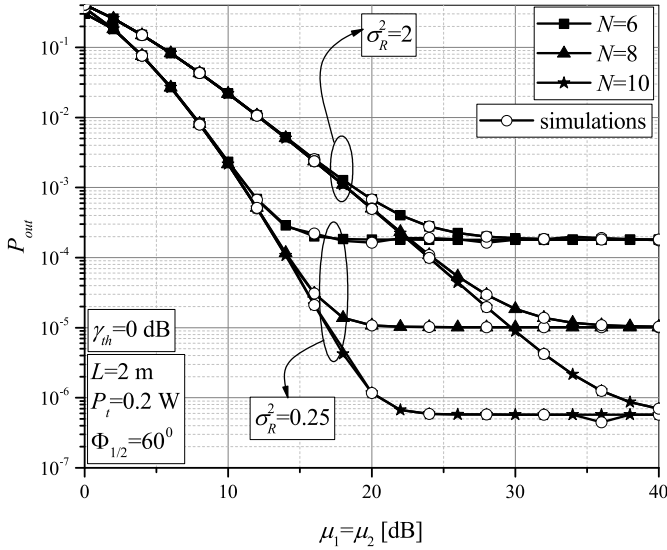


Fig. 4. Outage probability vs. $\mu_1 = \mu_2$ for different number of the VLC access points and various atmospheric turbulence strengths

access points can be 6, 8 or 10. As it is expected, system performs better when the FSO link suffers from weak turbulence conditions. Furthermore, in the range of medium and high $\mu_1 = \mu_2$ (greater RF signal power and greater FSO optical signal power), the overall system performance improvement is noticed when the number of available VLC channels is greater. In the range of low values of $\mu_1 = \mu_2$, the number of the VLC channels will not have impact on the system performance. In this scenario, the first sub-system will be in outage due to low transmitted power, thus the second system conditions improvement will not affect overall system performance.

Outage probability dependence on $\mu_1 = \mu_2$ for different values of LED output optical power, as well as different indoor

environment height, is depicted in Fig. 5. With greater LED radiation of the optical power, system performs better, but the cost and power consumption of the system is greater. It can be observed that the system performance is improved with lower dimension of the room height. When L is greater, the propagation path of the optical signal is longer, thus the total received power at the photodetector is reduced.

In both Fig. 4 and Fig. 5 the existence of the outage probability floor is noticed in the range of greater values of $\mu_1 = \mu_2$. When transmitted LED output power is constant, at some point, further increase of the RF or FSO signal power will not lead to the outage performance improvement. This outage probability floor appears at lower values of $\mu_1 = \mu_2$ when LED output power is lower, when the indoor space height is greater, as well as when N is lower and in weak turbulence conditions. This outage floor is limiting factor, thus, having high importance for RF/FSO-VLC system design.

V. CONCLUSION

In this paper, the analysis of the asymmetric relaying system, which was used to ensure traffic delivery to end users by indoor VLC multiple access points, was presented. The outdoor sub-system was hybrid RF/FSO system with SC diversity technique. Closed-form outage probability was derived and used to obtain numerical results, which were validated by Monte Carlo simulations. Various effects of system parameters on the outage probability performance were discussed.

It was presented that considered system performs better than the system when the first sub-system is a single FSO link, especially in strong atmospheric turbulence conditions. Number of available VLC access points determine the system performance to large extent. The outage probability floor was noticed, which is of high importance for system design and

implementation. It was proved that greater LED output power improves system performance, but in expense of the energy and cost savings.

ACKNOWLEDGMENT

This work has received funding from the European Union Horizon 2020 research and innovation programme under the Marie Skłodowska-Curie grant agreement No 734331. The paper was supported in part by the Ministry of Education, Science and Technology Development of the Republic of Serbia under grant TR-32035.

REFERENCES

- [1] L. C. Andrews and R. N. Philips, *Laser Beam Propagation through Random Media*. 2nd ed., Washington, USA: Spie Press, 2005.
- [2] Z. Ghassemlooy, W. Popoola, and S. Rajbhandari, *Optical Wireless Communications: System and Channel Modelling With MATLAB*. Boca Raton, FL, USA: CRC Press, 2013.
- [3] M. A. Khalighi and M. Uysal, "Survey on free space optical communication: A communication theory perspective," *IEEE Commun. Surveys Tuts.*, vol. 16, no. 4, pp. 2231–2258, Fourthquarter 2014.
- [4] Z. Ghassemlooy, L. N. Alves, S. Zvanovec, and M. A. Khalighi, (Eds.). *Visible Light Communications: Theory and Applications*. Boca Raton, FL, USA: CRC Press, 2017.
- [5] T. Komine and M. Nakagawa, "Fundamental analysis for visible-light communication system using LED lights," *IEEE Trans. Consum. Electron.*, vol. 50, no. 1, pp. 100–107, Feb. 2004.
- [6] A. Gupta, N. Sharma, P. Garg, and M.-S. Alouini, "Cascaded FSO-VLC communication system," *IEEE Wireless Commun. Lett.*, vol. 6, no. 6, pp. 810–813, Dec. 2017.
- [7] N. D. Chatzidiamantis, G. K. Karagiannidis, E. E. Kriezis, and M. Matthaiou, "Diversity combining in hybrid RF/FSO systems with PSK modulation," in *Proc. 2011 ICC*, Kyoto, pp. 1–6.
- [8] B. He and R. Schober, "Bit-interleaved coded modulation for hybrid RF/FSO systems," *IEEE Trans. Commun.*, vol. 57, no. 12, pp. 3753–3763, 2009.
- [9] M. K. Simon and M.-S. Alouni, *Digital Communication over Fading Channels*. 2nd ed., New York, NY: John Wiley & Sons Inc., 2004.
- [10] I. S. Gradshteyn and I. M. Ryzhik, *Table of Integrals, Series, and Products*. 6th ed., New York: Academic, 2000.
- [11] D. A. Basnayaka and H. Haas, "Design and analysis of a hybrid radio frequency and visible light communication system," *IEEE Trans. Commun.*, vol. 65, no. 10, pp. 4334 – 4347, Oct. 2017.
- [12] L. Yin, W. O. Popoola, X. Wu, and H. Haas, "Performance evaluation of non-orthogonal multiple access in visible light communication," *IEEE Trans. Commun.*, vol. 64, no. 12, pp. 5162–5175, Dec. 2016.
- [13] H. Marshoud, P. C. Sofotasios, S. Muhaidat, G. K. Karagiannidis, and B. S. Sharif, "On the performance of visible light communication systems with non-orthogonal multiple access," *IEEE Trans. Wireless Commun.*, vol. 16, no. 10, pp. 6350–6364, Oct. 2017.